Direction of Arrival Estimation Based on Phase Differences Using Neural Fuzzy Network

Ching-Sung Shieh and Chin-Teng Lin, *Senior Member, IEEE*

***Abstract*—A new high-resolution direction of arrival (DOA) estimation technique using a neural fuzzy network based on phase difference (PD) is proposed in this paper. The conventional DOA estimation method such as MUSIC and MLE, are computationally intensive and difficult to implement in real time. To attach these problems, neural networks have become popular for DOA estimation in recent years. However, the normal neural networks such as multilayer perceptron (MLP) and radial basis function network (RBFN) usually produce the extra problems of low convergence speed and/or large network size (i.e., the number of network parameters is large). Also, the way to decide the network structure is heuristic. To overcome these defects and take use of neural learning ability, a powerful self-constructing neural fuzzy inference network (SONFIN) is used to develop a new DOA estimation algorithm in this paper. By feeding the PD's of received radar-array signals, the trained SONFIN can give high-resolution DOA estimation. The proposed scheme is thus called PD-SONFIN. This new algorithm avoids the need of empirically determining the network size and parameters in normal neural networks due to the powerful on-line structure and parameter learning ability of SONFIN. The PD-SONFIN can always find itself an economical network size in fast learning process. Our simulation results show that the performance of the new algorithm is superior to the RBFN in terms of convergence accuracy, estimation accuracy, sensitivity to noise, and network size.**

***Index Terms*—Adaptive array, direction of arrival, fuzzy rule, membership function, multilayer perceptron network, neural fuzzy network, phase difference, radial basis function network, supervised learning.**

I. Introduction

THE problem of estimation is encountered in many areas such as radar, sonar, communication, and electronic surveillance. High-resolution direction-of-arrival (DOA) estimation at antenna arrays has been an extremely significant electronics support (ES) activity in both electronic warfare (EW) system and mobile communication systems for a long time. In EW application, since the DOA is obtained from the location of the input signal, this is the only parameter a hostile emitter cannot change easily [1]. Thus, the DOA becomes the most reliable and powerful sorting parameter. Nowadays, advanced radar intentionally irregularly varies radio frequency (RF), pulse repetition interval (PRI), and pulse width (PW), which can be controlled by a computer such that the radar signal is not easily intercepted and interfered. It is obvious that in highly dense signal environments, using electronic parameters such as RF, PRI, and PW to de-interleave is not a proper method. In mobile communication, once the direction of the users is detected, this information can be used in conjunction with any adaptive array technique so that the radiation pattern of the array is adapted to allocate the main beam toward the mobiles of interest while other sources of jamming in the same frequency slot are nulled and the communication system is able to track these mobiles in real time. Therefore, the accuracy of DOA manifests very important electronic parameter in interception of signal classification.

To handle the DOA estimation problem, some methods are proposed in [2], [3] such as autoregressive/moving average (AR/MA) and maximum entropy (ME); however, these methods have certain underlying limitations (either inability to resolve closely located sources or bias and sensitivity in parameter estimates) in light of using an inadequate model (e.g., AR rather than special ARMA model) [4]. High-resolution methods such as Pisarenko's and multiple signal classification (MUSIC) [5], [6] provide a reasonable approximation solution, but they are highly sensitive to the structure of the covariance matrix and require excessively large computation effort based on eigen-decomposition of data covariance matrix and as a result they are difficult to implement in real time. The ESPRIT [7], [8] method offers advantages over MUSIC algorithm by avoiding the orthogonality search and reducing the effect of sensor variability on the performance of the algorithm. However, this is achieved at the expense of increased number of sensors in the arrays [9]. This requirement generates production and maintenance costs that are increasingly prohibitive for many practical military applications. These abovementioned methods need to model signal and noise, so they are very sensitive to imperfections.

Neural networks have recently drawn a great deal of attention in many practical signal processing problems [9], [10] for the sake of their massive parallelism and global connectivity. The problem of DOA estimation is viewed as a potential application of neural networks, where such a problem is mapped onto the quadratic energy function for the Hopfield network to obtain the optimum estimate [9]. The DOA estimation problem can be also considered as a mapping from the space of DOA (θ) to the space of comparison system outputs (true phase differences $\boldsymbol{x}$) as in $\boldsymbol{x} = g(\theta)$. Then the DOA can be obtained via the inverse of this mapping directly, i.e., $\theta = f(\boldsymbol{x}) = g^{-1}(\boldsymbol{x})$. Park and Sanderberg proved the radial basis function network (RBFN) with one hidden layer was capable of universal approximation [11]. Thus, a RBFN was proposed to approximate the unknown

Manuscript received March 22, 1999; revised September 6, 1999. This work was supported by the National Science Council, R.O.C., under Grant NSC 89-2218-E-009-041.

The authors are with the Department of Electrical and Control Engineering, National Chiao-Tung University, Hsinchu 300, Taiwan, R.O.C. (e-mail: ctlin@fnn.cn.nctu.edu.tw).

Publisher Item Identifier S 0018-926X(00)06931-3.

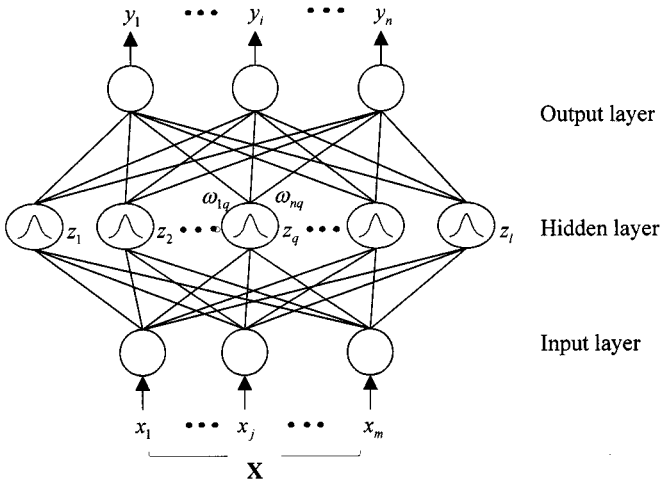

Fig. 1. Structure of the RBFN.

mapping function f such that whenever the available phase differences were fed into the network, the estimated DOA could be obtained from the output of the network [12]. In [13], a RBFN was used to handle the computational problem of the DOA estimation and the spatial correlation matrix was used as network input. In the RBFN, the input data undergo a nonlinear transformation through the basis functions in the network hidden layer. Then, the responses of basis functions are linearly combined to give the network output. Fig. 1 is a schematic diagram of the RBFN. Hence, the overall input–output transfer function of the RBFN has the form

$$y_i = a_i\left(\sum_{q=1}^{\ell}\omega_{iq}z_q + \theta_i\right) \tag{1}$$

$$z_q = g_q(\boldsymbol{x}) \triangleq \frac{\boldsymbol{R}_q(\boldsymbol{x})}{\sum_{k=1}^{\ell}\boldsymbol{R}_k(\boldsymbol{x})} = \frac{\exp\left[-|\boldsymbol{x}-\boldsymbol{m}_q|^2/2\sigma_q^2\right]}{\sum_{k=1}^{\ell}\exp\left[-|\boldsymbol{x}-\boldsymbol{m}_k|^2/2\sigma_k^2\right]} \tag{2}$$

where

$a_i(\bullet)$	output activation function;
θ_i	threshold value;
$\boldsymbol{x}$	input vector;
$\boldsymbol{m}_q$ and σ_q	mean (an m-dimensional vector) and variance of the qth Gaussian function;
ω_{iq}	network adjustable weights connecting network hidden nodes with network output;
z_q	qth hidden node which has normalized Gaussian activation function.

Generally, $a_i(\bullet)$ is an identity function (i.e., the output node is a linear unit) and $\theta_i = 0$. Methods of training the RBFN are beyond the scope of this paper; however, a detailed description of RBFN training methods can be found in [14].

It has been shown that the RBFN with node-growing capability requires many hidden units (neurons) to achieve the convergence accuracy within an acceptable error margin for a massive number of input data in a high-dimensional space. Although the RBFN can overcome the large computation and high-cost problems in the conventional DOA estimation methods, it has a fundamental limitation; a large number of parameters (network weights) need to be tuned in order to reach good performance of estimation because all of input variables are fully connected to its hidden nodes.

To cope with the drawbacks encountered in the RBFNs, while still keeping their advantages, a new DOA estimation algorithm with a neural fuzzy network is proposed in this paper. This neural fuzzy network is called SONFIN (self-constructing neural fuzzy inference network) that we proposed previously in [15]. The SONFIN is a feedforward multilayer network that integrates the basic elements and functions of a traditional fuzzy system into a connectionist structure. In this connectionist structure, the input nodes represent the corrupted signal process and output nodes represent the desired signal process and, in the hidden layers, there are nodes functioning as membership functions (activation functions) and fuzzy logic rules (connection types). The proposed algorithm can find the proper fuzzy logic rules dynamically on the fly. Also the SONFIN can always find itself an economical network size in high learning speed and, therefore, can avoid the need of empirically determining the number of hidden layers and nodes in ordinary neural networks. Since the structure of the SONFIN is constructed from fuzzy IF-THEN rules, expert knowledge can be put into the network as *a priori* knowledge, which can usually increase its learning speed and estimation accuracy [16], [17]. These properties make SONFIN an attractive candidate for constructing an inverse mapping.

The SONFIN is applied to approximate the functional relationship between phase differences (PDs) and DOA in this paper and, thus, the proposed scheme is called the PD-SONFIN algorithm. Studies have shown that the received radar signal amplitude is not always a strong indicator of DOA; on the other hand, there is a strong relationship between relative sensor phases (phase differences) and DOA [10]. The absolute phase of the received signal at each sensor also contains nonessential information. However, these phase differences contain artificial discontinuities caused by phase transitions in received phase data which are measured from $-\pi$ radians to $+\pi$ radians. Discontinuities make it difficult for the neural network to learn the mapping from a small discrete set of training points. To deal with this difficulty, we take the sine and cosine transform of the phase differences as input vectors which are fed into the SONFIN to perform training and estimating tasks. Continuous data can be obtained from this preprocess. Simulation results show that the proposed scheme achieves higher accuracy by using much fewer network parameters than the RBFN on the DOA estimation problem.

The rest of this paper is organized as follows. Section II states the problem formulation, where the preprocessing of input data is also described. In Section III, the basic structure and function of the SONFIN is briefly introduced and then the PD-based SONFIN is proposed. Section IV describes the performance of DOA estimation either with or without additive phase errors for both SONFIN and RBFN. Conclusions are summarized in Section V.

II. Problem Formulation

This section briefly describes the DOA estimation problem and provides a scheme to handle the artificial discontin-

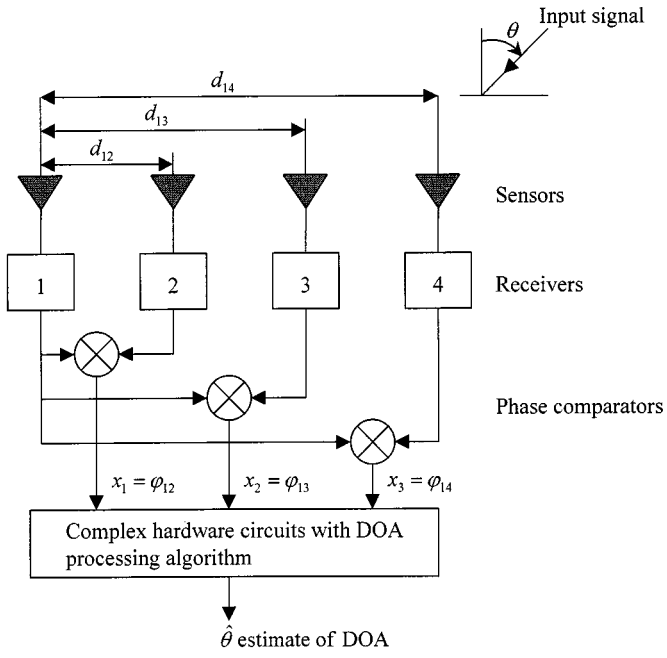

Fig. 2. Block diagram of the four-sensor comparison system.

uous problem caused by the measured phase transition. Many approaches have been proposed to measure input data corresponding to DOA information, where only amplitude comparison and phase comparison are the two most common approaches in EW applications. Amplitude-comparison approach is simple because the amplitude of an incident signal is relatively easy to measure over a wide frequency band. In contrast, phase-comparison approach is more accurate than amplitude-comparison approach. To enhance the estimation accuracy, our simulation results were achieved using the available phase differences only as input patterns of the DOA estimator in this paper. Naval Research Laboratory's report [18] indicates that the cascaded end-phase configurations of four-element sensors is optimum from the consideration of efficiency of hardware usage and probability of ambiguity. Hence, we select a four-element cascaded end-phase left configuration as the phase comparison system in our simulations. Goodwin in [18] describes that a four-element cascaded end-phase left interferometer can be characterized by four antenna/receiver channels, so three available channel-pair phase differences are necessary and sufficient to extract all the DOA-dependent electrical phase information. Fig. 2 shows the schematic diagram of this system; the channel at the far left side is the phase reference. We assume that a plane wave is coming in at incident angle θ from the boresight. Then the phase differences between a signal in the reference sensor and signals in the other sensors with additive phase errors can be well expressed by

$$\varphi_{1i} = 2\pi d_{1i} \sin\theta + \delta\varphi_{1i} \tag{3}$$

$$d_{1i} = \tfrac{1}{2} \sum_{j=1}^{i-1} L_j, \quad i = 2, 3, 4 \tag{4}$$

where

- φ_{1i} and $\delta\varphi_{1i}$ are the phase difference and phase error (noise) between the first sensor and the ith sensor, respectively;
- d_{1i} is the normalized physical spacing between the first sensor and the ith sensor, where the normalization is made with respect to the wavelength at the operating frequency;
- The adjacent sensor spacings (normalized to half-wavelengths at the operating frequency) are L_1 between sensors 1 and 2, L_2 between sensors 2 and 3, and L_3 between sensors 3 and 4;
- θ is direction of arrival.

According to the (3), once the phase differences are measured, the DOA can be determined through the complex hardware circuits with DOA processing algorithm. In conventional DOA estimation methods, the sensor spacing must be chosen optimally to achieve both low probability of ambiguity and high accurate estimates of DOA. As the phased-array sensors (antenna) become larger and more highly integrated into physical structures, this uniformity requirement generates production and maintenance costs that are increasingly prohibitive for many military and commercial applications. Because the conventional methods are cost consuming, a new approach is needed.

From a different point of view, the DOA estimation problem can be considered as a mapping from the space of DOA (θ) to the space of phase difference $(\boldsymbol{x})$ as $\boldsymbol{x} = g(\theta)$. Then the DOA can be obtained via the inverse of this mapping directly, i.e., $\theta = f(\boldsymbol{x}) = g^{-1}(\boldsymbol{x})$. An exactly closed-form formula for f cannot be obtained due to the high complexity of this mapping. Note that neural networks don't require any input calibration to correct the phase offset or sensor (antenna) mismatch. Thus, a RBFN was used to approximate the unknown mapping function f in [10], [12], and [13]. Once the available phase differences are fed into the network, the DOA estimate can be obtained from the network output directly. This is because the relationship between the input signal incident angle and the measured phase differences is generally a continuous function with small changes in angle yielding small changes in received measurements. The RBFN can solve the high costs (including production and maintenance costs) and computational complexity problems described above. However, in the RBFN used for DOA estimation, a large number of network parameters must be tuned to achieve high-estimation accuracy due to its structure. To solve this RBFNs defect and keep its advantages, we use a neural fuzzy network (SONFIN) to approximate the inverse mapping function f for DOA estimation in this paper. Hence, the input/output relationship of the DOA estimation problem can be denoted by

$$\hat{\theta} = \hat{f}(\boldsymbol{x}) \tag{5}$$

where

$\hat{\theta}$ estimated DOA;
$\hat{f}$ estimate of f;
$\boldsymbol{x}$ input data [i.e., phase differences φ_{1i}s in (3)].

Considering the multi-input single-output case for clarity, we assume that the number of the measured phase differences is m [i.e., input data $\boldsymbol{x} = (x_1, \ldots, x_m) = (\varphi_{12}, \ldots, \varphi_{1m+1})$], and the number of the estimation output is one. In general, the neural networks operate in two phases: training phase and testing phase. In the training phase, the training data pairs $(\boldsymbol{x}, f(\boldsymbol{x}))$ are generated from (3) with $\delta\varphi_{1i} = 0$, where $f(\boldsymbol{x})$ is

the function to be approximated. The objective of learning is to minimize the error function

$$E = \tfrac{1}{2}\left(y(t) - y^d(t)\right)^2 \tag{6}$$

where $y^d(t)$ is the network output (desired output) and $y(t)$ is the actual output (estimated DOA). The total number of training pairs is 181 in our simulations. In the testing phase, another set of data (301 patterns in our simulations) are derived from different signal conditions (either with or without additive phase errors) according to (3) and are used for testing. These testing data are fed into the trained network. Then the DOA can be estimated via this inverse mapping network directly.

In our simulations, we find that the input phase differences (φ_{1i}, $i = 1, \ldots, m+1$) contain artificial discontinuities due to the fact that each member of the ensemble of phase comparator outputs can only be known as modulo 2π. The discontinuous training patterns make both the SONFIN and RBFN difficult to perform the learning task successfully. To eliminate the irrelevant artificial discontinuities, we adopt the *in-phase* and the so-called *quadrature* representation of input signals by using the sine and cosine transform of phase differences as network inputs. According to this representation, the original input vector containing m phase differences $x_1, x_2, \ldots, x_m$ are transformed into the following enlarged vector:

$$\Phi = (\phi_1, \phi_2, \ldots, \phi_{2m}) \in [-1, 1]^{2m} \tag{7}$$

where

$\phi_1 = \sin(x_1), \ldots;$
$\phi_m = \sin(x_m),$
$\phi_{m+1} = \cos(x_1), \ldots;$
$\phi_{2m} = \cos(x_m).$

Our simulation results showed that if we used these processed data as the inputs of neural networks (either RBFN or SONFIN) directly, we obtained satisfactory convergent accuracy.

III. Estimation of DOA Using a Neural Fuzzy Network

In this section, we shall introduce a neural fuzzy network and then propose a high-resolution DOA estimation scheme based on this network with the phase differences as input patterns.

A. Self-Constructing Neural Fuzzy Inference Network (SONFIN)

The neural fuzzy network that we used for DOA estimation is the so-called SONFIN that we proposed previously in [15]. The SONFIN is a general connectionist model of a fuzzy logic system, which can find its optimal structure and parameters automatically. There are no rules initially in the SONFIN. They are created and adapted as on-line learning proceeds via simultaneous structure and parameter learning, so the SONFIN can be used for normal operation at any time as learning proceeds without any assignment of fuzzy rules in advance. A novel network construction method for solving the dilemma between the number of rules and the number of consequent terms is developed. The number of generated rules and membership functions is small even for modeling a sophisticated system. The SONFIN always produces an economical networks size and the learning speed and modeling ability are superior to ordinary neural networks.

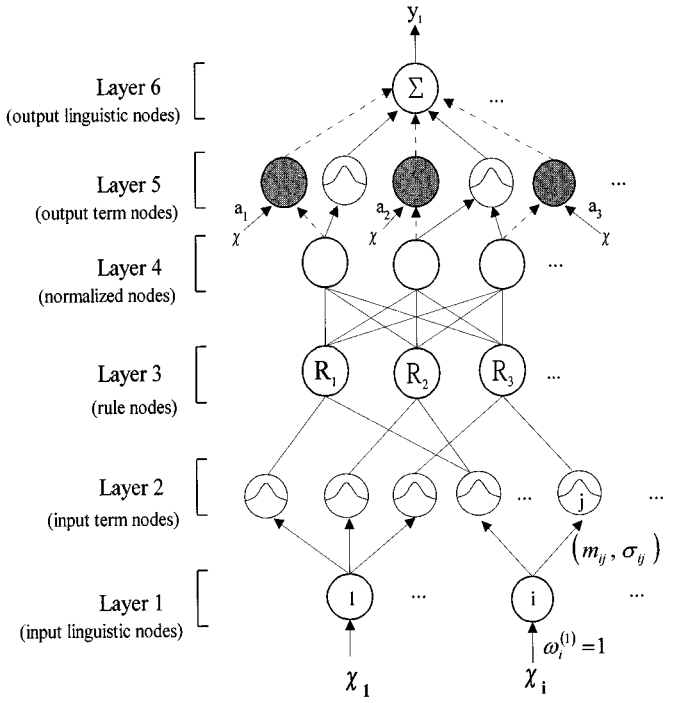

Fig. 3. Structure of the SONFIN.

A key feature of the SONFIN structure is that a high-dimensional fuzzy system is implemented with small number of rules and fuzzy terms. This is achieved first by partitioning the input and output spaces into clusters efficiently through learning proper fuzzy terms for each input/output variable, and then by constructing fuzzy rules optimally through finding proper mapping between input and output clusters in the SONFIN. In addition, due to the physical meaning of fuzzy IF-THEN rule, each input node in the SONFIN is only connected to its related rule nodes through its term nodes, instead of being connected to *all* the rule nodes in Layer 3 of the SONFIN. This results in a small number of weights to be tuned in the SONFIN. In contrast, each input node in the RBFN is fully connected to hidden nodes, whose number is usually large as compared to the number of rule nodes learned in the SONFIN in order to reach good performance of estimation. This usually leads to a large number of weights to be tuned in the RBFN.

The structure of the SONFIN is shown in Fig. 3. This six-layered network realizes a fuzzy model of the following form:

$$\text{Rule } i\text{: IF } x_1 \text{ is } A_1^i \text{ and } \ldots \text{ and } x_n \text{ is } A_n^i$$
$$\text{THEN } y \text{ is } m_0^i + a_j^i x_j + \ldots$$

where

A_j^i fuzzy set of the ith linguistic term of input variable x_j;
m_0^i center of a symmetric membership function on y;
a_j^i consequent parameter.

It is noted that unlike the traditional Takagi–Sugeno–Kang (TSK) model where all the input variables are used in the output linear equation, only the significant ones are used in the SONFIN; i.e., some a_j^is in the above fuzzy rules are zero. We shall next describe the functions of the nodes in each of the six layers of the SONFIN.

The SONFIN consists of nodes, each of which has some finite fan-in of connections represented by weight values from other nodes and fan-out of connections to other nodes. Associated with the fan-in of a node is an integration function f which serves to combine information, activation, or evidence from other nodes. This function provides the net input for this node

$$\text{net}_{\text{input}} = f\left(u_1^{(k)}, u_2^{(k)}, \ldots, u_p^{(k)}; w_1^{(k)}, w_2^{(k)}, \ldots, w_p^{(k)}\right)$$

where $u_1^{(k)}, u_2^{(k)}, \ldots, u_p^{(k)}$ are inputs to this node, and $w_1^{(k)}, w_2^{(k)}, \ldots, w_p^{(k)}$ are the associated link weights. The superscript (k) in the above equation indicates the layer number. This notation will also be used in the following equations. A second action of each node is to output an activation value as a function of its $\text{net}_{\text{input}}$

$$\text{output} = o_i^{(k)} = a(\text{net}_{\text{input}}) = a(f)$$

where $o_i^{(k)}$ denotes the output of the ith node in the layer k, and $a(\cdot)$ denotes the activation function. We shall describe the functions of the nodes in each of the six layers of the SONFIN as follows.

Layer 1: No computation is done in this layer. Each node in this layer, which corresponds to one input variable, only transmits input values to the next layer directly. That is

$$f = u_i^{(1)} \text{ and } a^{(1)} = f. \tag{8}$$

From the above equation, the link weight in layer one $(w_i^{(1)})$ is unity.

Layer 2: Each node in this layer corresponds to one linguistic label (small, large, etc.) of one of the input variables in Layer 1. In other words, the membership value, which specifies the degree to which an input value belongs to a fuzzy set is calculated in Layer 2. With the choice of Gaussian membership function, the operation performed in this layer is

$$f_j\left(u_i^{(2)}\right) = -\frac{\left(u_i^{(2)} - m_{ij}\right)^2}{\sigma_{ij}^2} \text{ and } a^{(2)}(f) = e^f \tag{9}$$

where m_{ij} and σ_{ij} are, respectively, the center (or mean) and the width (or variance) of the Gaussian membership function of the jth partition for the ith input variable u_i. Hence, the link weight in this layer can be interpreted as m_{ij}.

Layer 3: A node in this layer represents one fuzzy logic rule and performs precondition matching of a rule. Here, we use the following AND operation for each Layer-3 node:

$$f\left(u_i^{(3)}\right) = \prod_{i=1}^{q} u_i^{(3)} = e^{-[D_i(\boldsymbol{x}-\boldsymbol{m}_i)]^T[D_i(\boldsymbol{x}-\boldsymbol{m}_i)]} \text{ and } a^{(3)}(f) = f \tag{10}$$

where

- q number of Layer-2 nodes participating in the IF part of the rule;
- D_i diag $(1/\sigma_{i1}, 1/\sigma_{i2}, \ldots, 1/\sigma_{in})$;
- $\boldsymbol{m}_i$ $(m_{i1}, m_{i2}, \ldots, m_{in})^T$.

The weights of the links in Layer 3 $(w_i^{(3)})$ have the value of one. The output f of a Layer-3 node represents the firing strength of the corresponding fuzzy rule.

Layer 4: The number of nodes in this layer is equal to that in Layer 3 and the firing strength calculated in Layer 3 is normalized in this layer by

$$f\left(u_i^{(4)}\right) = \sum_{i=1}^{r} u_i^{(4)} \text{ and } a^{(4)}(f) = u_i^{(4)}/f \tag{11}$$

where r is the number of rule nodes in Layer 3. Like Layer 3, the link weight $(w_i^{(4)})$ in this layer is unity, too.

Layer 5: This layer is called the consequent layer. Two types of nodes are used in this layer and they are denoted as blank and shaded circles in Fig. 3, respectively. The node denoted by a blank circle (blank node) is the essential node representing a fuzzy set (described by a Gaussian membership function) of the output variable. Only the center of each Gaussian membership function is delivered to the next layer for the LMOM (local mean of maximum) defuzzification operation and the width is used for output clustering only. Different nodes in Layer 4 may be connected to a same blank node in Layer 5, meaning that the same consequent fuzzy set is specified for different rules. The function of the blank node is

$$f = \sum_{i=1}^{s} u_i^{(5)} \text{ and } a^{(5)}(f) = f \cdot a_0^i \tag{12}$$

where s is the number of nodes in Layer 4 and $a_0^i = m_0^i$ is the center of a Gaussian membership function. As to the shaded node, it is generated only when necessary. Each node in Layer 4 has its own corresponding shaded node in Layer 5. One of the inputs to a shaded node is the output delivered from Layer 4 and the other possible inputs (terms) are the input variables from Layer 1. The shaded node function is

$$f = \sum_{j=1}^{n} a_j^i x_j \text{ and } a^{(5)}(f) = f \cdot u_i^{(5)} \tag{13}$$

where the summation is over the significant terms connected to the shaded node only and a_j^i is the corresponding parameter. Combining these two types of nodes in Layer 5, we obtain the whole function performed by this layer as

$$a^{(5)}(f) = \left(\sum_{j=1}^{n} a_j^i x_j + a_0^i\right) u_i^{(5)}. \tag{14}$$

Layer 6: Each node in this layer corresponds to one output variable. The node integrates all the actions recommended by Layer 5 and acts as a defuzzifier with

$$f\left(u_i^{(6)}\right) = \sum_{i=1}^{t} u_i^{(6)} \text{ and } a^{(6)}(f) = f \tag{15}$$

where t is the number of nodes in Layer 5.

Two types of learning (structure and parameter learning) are used concurrently for constructing the SONFIN. The structure learning includes both the precondition and consequent structure identification of a fuzzy IF-THEN rule. Here the precondition structure identification corresponds to the input-space partitioning and can be formulated as a combinational optimization problem with the following two objectives: to minimize the number of rules generated and to minimize the number of fuzzy sets on the universe of discourse of each input variable. As to the consequent structure identification, the main task is to decide when to generate a new membership

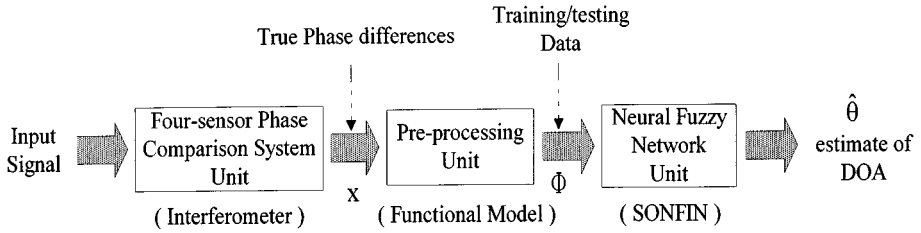

Fig. 4. Flow chart of DOA estimation using the SONFIN.

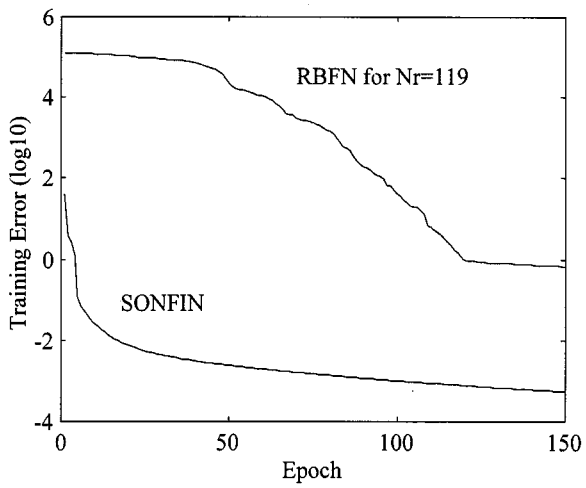

Fig. 5. Convergence curves of the SONFIN and RBFN.

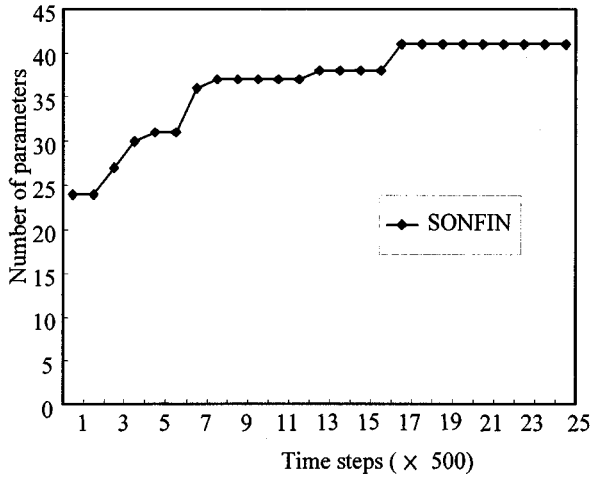

Fig. 6. Structure-growing curve indicating the increasing of parameter number of the SONFIN during its learning process.

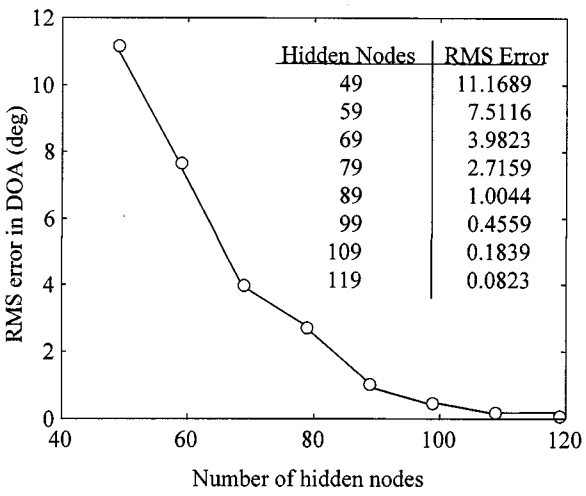

Fig. 7. Effect of the number of hidden nodes in the RBFN on rms error.

function for the output variable and which significant terms (input variables) should be added to the consequent part (a linear equation) when necessary. For the parameter learning, based upon supervised learning algorithms, the parameters of the linear equations in the consequent parts are adjusted by either least mean squares (LMS) or recursive least squares (RLS) algorithms, and the parameters in the precondition part are adjusted by the backpropagation algorithm to minimize a given cost function. The SONFIN can be used for normal operation at any time during the learning process without repeated training on the input/output patterns when on-line operation is required. There are no rules (i.e., no nodes in the network except the input/output nodes) in the SONFIN initially. They are created dynamically as learning proceeds upon receiving on-line incoming training data by performing the following learning processes simultaneously: A) input/output space partition; B) construction of fuzzy rules; C) optimal consequent structure identification; D) parameter identification. In the above, processes A, B, and C belong to the structure learning phase and process D belongs to the parameter learning phase.

In the structure identification of the precondition part of the SONFIN, the input space is partitioned in a flexible way according to an aligned clustering-based algorithm. As to the structure identification of the consequent part, only a singleton value selected by a clustering method is assigned to each rule initially. Afterwards, some additional significant terms (input variables) selected via projected-based correlation measure for each rule will be added to the consequent part (forming a linear equation of input variables). The combined precondition and consequent structure identification scheme can set up an economical and dynamically growing network automatically. This makes the SONFIN can grow its rule nodes, term nodes, and link weights upon necessary on the fly and, thus, own the so-called *self-construction* capability. The details of the learning processes for SONFIN are described in [15].

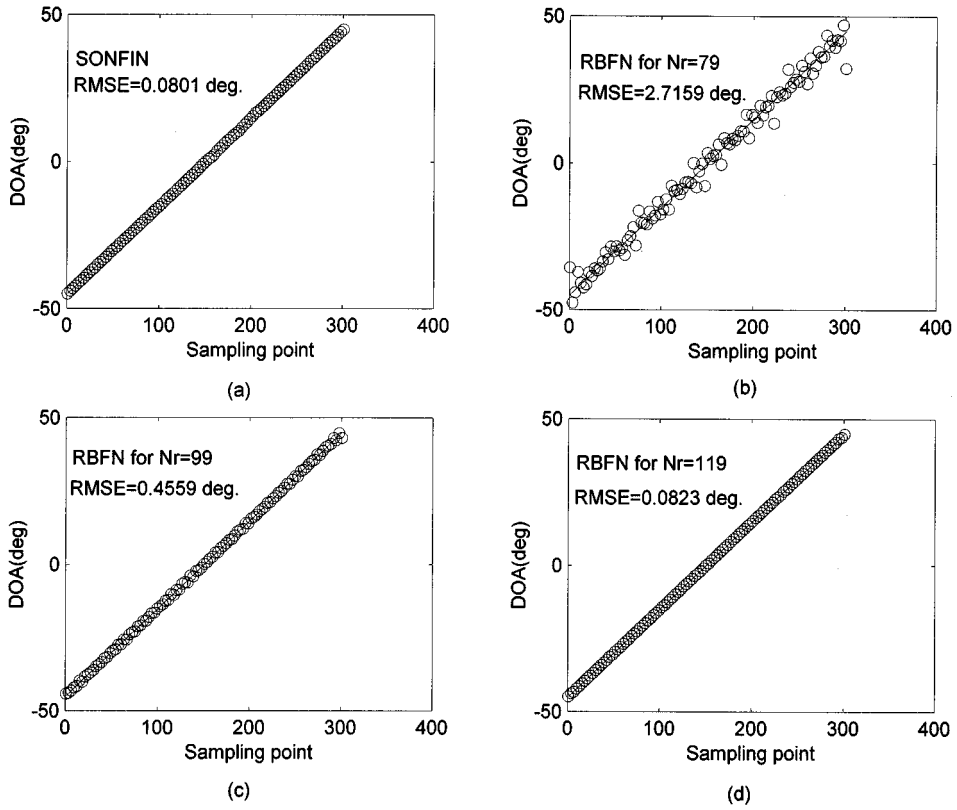

Fig. 8. (a) Testing results of the trained SONFIN estimator, where the desired output is shown by solid line "–," and the actual network output by circle "o." (b), (c), and (d) Testing results of the trained RBFN estimator $N_r = 79,\ 99,\ 119$, where the desired output is shown by solid line "–," and the actual network output by circle "o."

B. PD-SONFIN for DOA Estimation

Fig. 4 shows the flow chart of DOA estimation using SONFIN based on channel-pair phase differences. The configuration of the proposed DOA estimation scheme is composed of the following units.

1) *Phase comparison unit* (interferometer), which is used to measure the phase differences.
2) *Preprocessing unit* (functional model), which is used to eliminate the artificial discontinuities caused by phase transitions as mentioned Section II.
3) *Neural fuzzy network prediction unit* (SONFIN), which is to estimate the DOA from the preprocessed phase differences.

The operation takes place as follows. First, we assume an $(m+1)$-element sensor system. From the phase comparison unit, we can obtain m-dimensional phase difference vectors, $(x_1, x_2, \cdots, x_m)$, which are preprocessed to eliminate artificial discontinuities. After preprocessing, it will generate $2m$-dimensional enlarged vectors, $\Phi = (\phi_1, \phi_2, \cdots, \phi_{2m})$, which are the real inputs to the DOA estimation network, SONFIN. Before entering the SONFIN, a normalization process is used to rescale each enlarged $2m$-dimensional vector in $[-1, 1]^{2m}$ to a $2m$-dimensional vector in $[0, 1]^{2m}$. Due to the property of SONFIN, all the training and testing vectors need to be normalized to the range of [0, 1]. The normalized vectors are put into the SONFIN for training. In the training phase, the SONFIN is trained by the input/output pairs $(\Phi, f(\Phi))$. Then the trained SONFIN is ready for DOA estimation. Once each input vector (corresponding to a DOA value) is given, the output node in Layer 6 of the SONFIN indicates directly a DOA estimate. In the testing phase, all the testing data are processed through the same preprocessing and normalization procedures. After feeding the processed data into the trained SONFIN, we can obtain the estimated DOA values from the output node of SONFIN.

IV. Simulation Results

This section illustrates the performance of the proposed DOA estimator either with or without additive phase errors. The simulations are conducted by emulating the physical antenna (coverage 2 GHz ∼4 GHz) deployed in our real system. In our system, a four-element cascaded end-phase left interferometer is used to generate three phase differences. We take sine and cosine transformation of three phase differences as network inputs. The system performance is verified for input signal with frequency 2.702 GHz. The optimal sensor spacing for high DOA estimation accuracy was chosen based on the theoretical analysis given in [18]. Our previous verification results showed that the physical antenna deployed was realizable and the DOA estimation accuracy reached the highest value when the sensor spacing was chosen as $L_1 = 9$, $L_2 = 6$, and $L_3 = 7$ times of half wavelengths at reference frequency 4 GHz. This previous study was performed by using conventional DOA estimation technique through complex hardware with digital signal

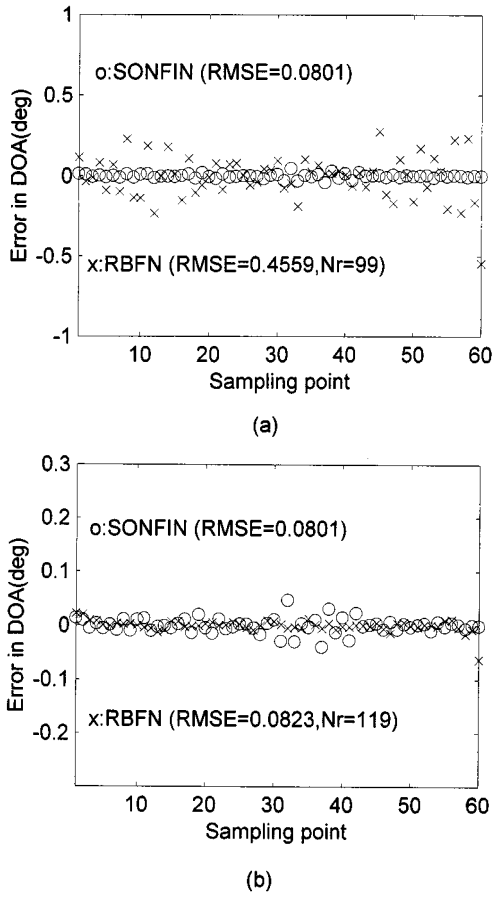

Fig. 9. (a) DOA estimation error comparison between the RBFN (with $N_r = 99$) and SONFIN. (b) DOA estimation error comparison between the RBFN (with $N_r = 119$) and SONFIN.

processing program. We thus adopt the above parameters in the simulations of this paper.

A. Performance of DOA Estimation Without Phase Errors

In the absence of additive phase errors, (3) and (4) can be written as

$$\varphi_{1i} = 2\pi d_{1i} \sin\theta \tag{16}$$

$$d_{1i} = \tfrac{1}{2} \sum_{j=1}^{i-1} L_j,\ i = 2, 3, 4. \tag{17}$$

By empirical information, the DOA estimates at intervals from -45° to $+45^\circ$ are sufficient in the real scenario. Hence, the training data are generated as follows. We divide the range of DOA values, -45 to $+45$, equally into 180 intervals, with each interval being 0.5°. As a result, we have 181 DOA values in the set $\{-45.0, -44.5, \cdots, +44.5, +45\}$. In Fig. 2, the interferometer receives a single source. Then we calculate the three phase-difference values, φ_{12}, φ_{13}, φ_{14}, corresponding to each of these DOA values from (16) and (17). Through the preprocessing and normalization units, each three-element phase-difference vector is transformed into a six-element vector. The pair of a six-element vector and the corresponding DOA value form a training pattern in the form of (input, desired output). Hence, as a total, we have 181 training patterns. With the same procedure, we can obtain 301 (input, desired output) pairs as testing patterns by dividing the range of DOA values, -45 to $+45$, into 0.3° intervals. In our simulations, the same training and testing data sets are fed into the SONFIN and RBFN for DOA estimation.

TABLE I
PERFORMANCE COMPARISON OF THE SONFIN AND RBFN ESTIMATORS ON THE DOA ESTIMATION PROBLEM

Methods	SONFIN	RBFN		
		Nr=79	Nr=99	Nr=119
Estimation Accuracy (degree)	0.0801	2.7159	0.4559	0.0823
Number of nodes	57	86	106	126
Number of parameters	41	1027	1287	1547

In the training phase, after 150 epochs of learning, the converged root mean squared (rms) error of the SONFIN is below 10^{-3}, but that of the RBFN is only below one. Fig. 5 shows the convergence curves of the RBFN and SONFIN, respectively. The convergence rate of the SONFIN is much higher than that of the RBFN. The structure-growing curve of the SONFIN is given in Fig. 6, which indicates the on-line self-construction capability of the SONFIN as learning proceeds. The rms error in DOA of the RBFN with respect to the number of hidden nodes (Nr) is shown in Fig. 7. To further reduce the rms error, we must increase the number of hidden nodes.

In the testing phase, the DOAs obtained from the SONFIN and those from the RBFN with different hidden node numbers (Nr $= 79$, Nr $= 99$, or Nr $= 119$) are shown in Fig. 8. The testing results show that the SONFIN successfully produced actual output "o" very close to the desired DOA "–," For comparison, the errors in DOA estimation obtained from the SONFIN and those from the RBFN are plotted in Fig. 9. For this example case, the simulation results show that the required number of tunable parameters in the SONFIN is about 1/37 time of that in the RBFN under the same rms error condition. A detailed performance comparisons are listed in Table I.

B. Performance of DOA Estimation with Phase Errors

In this simulation, the training was performed with 181 data sets derived from (16) and (17) (assuming the absence of phase errors), whereas the testing was performed with 301 data sets contaminated with uniformly distributed phase errors derived

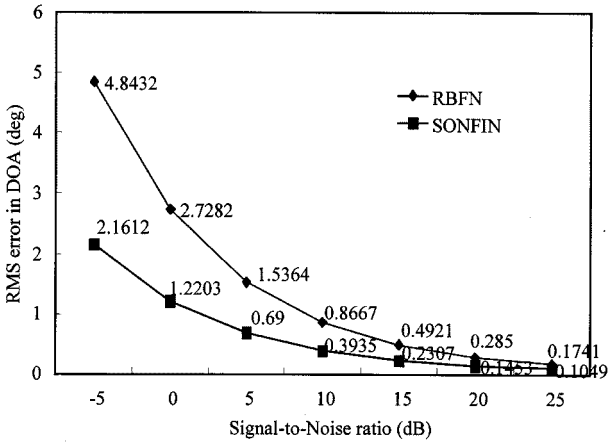

Fig. 10. RMS error in DOA of the SONFIN and RBFN ($N_r = 119$) under the additive phase error conditions with different SNRs.

from (3) and (4) to simulate real measurements. In (3), the additive phase error (noise) term is given by

$$\delta\varphi_{1i} = \frac{\sigma_\phi}{\sqrt{2}\pi d_{1i}}, \quad i = 2, 3, 4 \tag{18}$$

$$\sigma_\phi = \frac{180^\circ}{\pi\sqrt{\text{SNR}}} \tag{19}$$

where signal-to-noise ratio (SNR) is in terms of power. The above additive phase error (noise) term is given by references [1], [18] . For comparison, the errors in DOA estimation obtained from the SONFIN and those from the RBFN with additive phase errors at different signal-to-noise ratio values are plotted in Fig. 10. The simulation results show that the SONFIN outperforms the RBFN by yielding smaller rms errors in noisy environments. In conclusion, the SONFIN appears relatively more insensitive to noise than the RBFN.

V. Conclusion

In this paper, we have proposed a neural fuzzy scheme for estimating the direction of arrival of moving targets based on the phase differences from an interferometer. In addition, to avoid the discontinuities caused by the input phase transition, we use the quadrature representation of the phase differences. Unlike conventional eigen-based DOA estimator, the proposed scheme requires no large amount of computations and does not need to model signal. The main advantage of the proposed network (SONFIN) is that it always produces an economical networks size and the learning speed and modeling ability are superior to ordinary neural networks. Hence, the trained SONFIN automatically estimates DOA for different phase differences so that neither numerical methods nor graphical methods need to be used. We use two networks, RBFN and SONFIN, to estimate DOA at different SNR values (from -5 to 25 dB). Simulation results show that the SONFIN always produces actual output very close to the desired DOA values, and the required number of parameters in the SONFIN is about 1/37 time of that in the RBFN under the same rms error in DOA. Notice that this result of parameters reduction is based on the specific example presented in this paper, and is not a general conclusion that applies to all SONFIN/RBFN comparisons. With these results achieved in this paper, the proposed neural fuzzy scheme could be widely applied to military applications (such as reconnaissance and threat reaction) for achieving high accurate DOAs for certain electronics support measures. Especially, the proposed method can be applied to the problem of moving target tracking. As the targets move, their motion is tracked through a SONFIN which uses the data provided by the most recent output of the sensor array to update the existing estimate of target angles.

References

[1] B. Y. Tsui, *Microwave Receivers with Electronic Warfare Applications*. New York: Wiley, 1986.
[2] M. H. Hayes, *Statistical Digital Signal Processing and Modeling*. New York: Wiley, 1996.
[3] B. Widrow and S. D. Stearns, *Adaptive Signal Processing*. Englewood Cliffs, NJ: Prentice-Hall, 1985.
[4] S. M. Kay and S. L. Marple Jr., "Spectrum analysis—A modern perspective," *Proc. IEEE*, vol. 69, pp. 1380–1419, Nov. 1981.
[5] D. H. Johnson and S. R. DeGraaf, "Improving resolution of bearing in passive sonar arrays by eigenvalue analysis," *IEEE Trans. Acoust., Speech, Signal Processing*, vol. ASSP-30, pp. 638–647, Aug. 1982.
[6] R. O. Schmidt, "Multiple emitter location and signal parameter estimation," *IEEE Trans. Antennas Propagat.*, vol. AP-34, pp. 276–280, Mar. 1986.
[7] A. Paulraj and T. Kailath, "Eigenstructure methods for direction of arrival estimation in the presence of unknown noise fields," *IEEE Trans. Acoust., Speech, Signal Processing*, vol. ASSP-34, Feb. 1986.
[8] R. Roy and T. Kailath, "ESPRIT-estimation of signal parameters via rotational invariance techniques," *IEEE Trans. Acoust., Speech, Signal Processing*, vol. 37, no. 7, pp. 984–995, July 1989.
[9] S. Jha and T. S. Durrani, "Direction of arrival estimation using artificial neural networks," *IEEE Trans. Syst., Man, Cybern.*, vol. 21, no. 5, pp. 1192–1201, Sept./Oct. 1991.
[10] H. L. Southall, J. A. Simmers, and T. H. O'Donnell, "Direction finding in phased arrays with a neural network beamformer," *IEEE Trans. Antennas Propagat.*, vol. 43, pp. 1369–1374, Dec. 1995.
[11] J. Park and I. W. Sandberg, "Universal approximation using radial basis function networks," *Neural Computat.*, vol. 3, pp. 246–257, 1991.
[12] T. Lo, L. Henry, and L. John, "Radial basis function neural network for direction of arrivals estimation," *IEEE Signal Processing Lett.*, vol. 1, pp. 45–47, Feb. 1994.
[13] A. H. El Zooghby, C. G. Christodoulou, and M. Georgiopoulos, "Performance of radial-basis function networks for direction of arrival estimation with antenna arrays," *IEEE Trans. Antennas Propagat.*, vol. 45, pp. 1611–1617, Nov. 1997.
[14] S. Chen, C. F. N. Cowan, and P. M. Grant, "Orthogonal least squares learning algorithm for radial-basis function networks," *IEEE Trans. Neural Networks*, vol. 2, pp. 302–309, Mar. 1991.
[15] C. F. Juang and C. T. Lin, "An on-line self-constructing neural fuzzy inference network and its application," *IEEE Trans. Fuzzy Syst.*, vol. 6, pp. 12–32, Feb. 1998.
[16] C. T. Lin, *Neural Fuzzy Control Systems with Structure and Parameter Learning*. Singapore: World Scientific, 1994.
[17] C. T. Lin and C. S. G. Lee, *Neural Fuzzy Systems: A Neural-Fuzzy Synergism to Intelligent Systems*. Englewood Cliffs, NJ: Prentice-Hall, May 1996.
[18] L. Goodwin, "Ambiguity-resistant three and four channel interferometers," Naval Res. Lab. Rep. 8005, Sept. 1976.
[19] Y. H. Pao, *Adaptive Pattern Reconigition and Neural Networks*. Reading, MA: Addison-Wesley, 1989.

Ching-Sung Shieh received the B.S. and M.S. degrees in electronic engineering from the Chung-Yuan Christian University, Taoyuan, Taiwan, R.O.C., in 1984 and 1986, respectively. He is currently working toward the Ph.D. degree in the Department of Electrical and Control Engineering at the National Chiao-Tung University, Hsinchu, Taiwan.

From 1986 to 1996, he worked as an Assistant Researcher at the Chung-Shan Institute of Science and Technology (CSIST), Taiwan. His current research interests include radar signal processing, control systems design, neural networks, estimation theory, and applications.

Chin-Teng Lin (S'88–M'91–SM'99) received the B.S. degree in control engineering from the National Chiao-Tung University, Hsinchu, Taiwan, R.O.C., in 1986, and the M.S.E.E. and Ph.D. degrees in electrical engineering from Purdue University, West Lafayette, IN, in 1989 and 1992, respectively.

Since August 1992, he has been with the College of Electrical Engineering and Computer Science, National Chiao-Tung University, Hsinchu, Taiwan, R.O.C., where he is currently a Professor of electrical and control engineering. He also serves as the Deputy Dean of the Research and Development Office of the National Chiao-Tung University since 1998. He is the coauthor of *Neural Fuzzy Systems—A Neuro-Fuzzy Synergism to Intelligent Systems* (Englewood Cliffs, NJ: Prentice-Hall, 1996), and the author of *Neural Fuzzy Control Systems with Structure and Parameter Learning* (Singapore: World Scientific, 1994). He has published around 50 journal papers in the areas of neural networks and fuzzy systems. His current research interests are fuzzy systems, neural networks, intelligent control, human-machine interface, and video and audio processing.

Dr. Lin is a member of Tau Beta Pi and Eta Kappa Nu. He is also a member of the IEEE Computer Society, the IEEE Robotics and Automation Society, and the IEEE Systems, Man, and Cybernetics Society. He has been the Executive Council Member of Chinese Fuzzy System Association (CFSA) since 1995 and the Supervisor of Chinese Automation Association since 1998. He was the Vice Chairman of IEEE Robotics and Automation Taipei Chapter in 1996 and 1997. He won the Outstanding Research Award granted by National Science Council (NSC), Taiwan, in 1997 and 1999, the Outstanding Electrical Engineering Professor Award granted by the Chinese Institute of Electrical Engineering (CIEE) in 1997, and the Outstanding Engineering Professor Award granted by the Chinese Institute of Engineering, in 2000.